The role of adsorption in the catalytic electrode mechanism studied by means of square-wave voltammetry

ARTICLE *in* JOURNAL OF ELECTROANALYTICAL CHEMISTRY · APRIL 2005

Impact Factor: 2.73 · DOI: 10.1016/j.jelechem.2004.12.017

2 AUTHORS:

Valentin Mirceski
Ss. Cyril and Methodius University
102 PUBLICATIONS **1,600** CITATIONS

SEE PROFILE

François Quentel
Université de Bretagne Occidentale
106 PUBLICATIONS **1,063** CITATIONS

SEE PROFILE

Available online at www.sciencedirect.com
SCIENCE DIRECT®
Journal of Electroanalytical Chemistry 578 (2005) 25–35
Journal of Electroanalytical Chemistry
www.elsevier.com/locate/jelechem

The role of adsorption in the catalytic electrode mechanism studied by means of square-wave voltammetry

Valentin Mirčeski [a,*], François Quentel [b]

[a] Institute of Chemistry, Faculty of Natural Sciences and Mathematics, St. Cyril and Methodius University, P.O. Box 162, Archimedova 5, Skopje 1000, Republic of Macedonia

[b] Laboratoire de Chimie Analytique, UMR-CNRS 6521, Université de Bretagne Occidentale, 6, avenue Victor Le Gorgeu, C.S. 93837, 29238 BREST Cedex, France

Received 21 July 2004; received in revised form 1 December 2004; accepted 2 December 2004
Available online 5 February 2005

Abstract

A complex electrode mechanism coupled with adsorption of the redox couple and an irreversible homogeneous chemical reaction that regenerates the electroactive reactant is studied both theoretically and experimentally under conditions of square-wave voltammetry. The homogeneous regenerative redox reaction, i.e., the so-called catalytic reaction, takes place as a surface or volume process, depending on whether it includes the dissolved or adsorbed form of the electrode product, respectively. A rigorous theoretical model is presented considering simultaneously all relevant phenomena affecting the voltammetric response, such as mass transport, adsorption equilibria and kinetics of two different catalytic reactions, i.e., volume and surface catalytic reactions. The solutions for the surface concentration of the electroactive species are presented in the form of integral equations, thus they are general and valid for any chronoamperometric and voltammetric technique. The model enables systematic study of the role of adsorption in a complex catalytic electrode mechanism. The properties of the voltammetric response show remarkable discrepancies between the effect of the volume and surface catalytic reactions, thus enabling their recognition and separate characterization. From an analytical point of view it is demonstrated that the catalytic mechanism of moderate adsorption is superior in comparison with the pure volume and surface catalytic mechanisms. The theoretical predictions are confirmed by the voltammetric behaviour of the redox couple azobenzene/hydrazobenzene at the mercury electrode by using a mixture of water + acetonitrile as a solvent.

Keywords: Square-wave voltammetry; Catalytic reaction; Adsorption; Mathematical modelling

1. Introduction

The cyclic electrode mechanism in which the product of the electrode reaction is turned back into the electroactive reactant by means of a homogeneous redox chemical reaction is called a catalytic electrode mechanism (see Scheme 1(A)). Though the term "catalytic" is partly ambiguous, it probably stems from the fact that the voltammetric response of such an electrode reaction is larger than in the absence of the homogeneous redox reaction, as well as that it increases in proportion with the rate of the latter reaction. Three aspects of the catalytic electrode reactions are of particular importance. First, catalytic electrode mechanisms are the basis for studying the thermodynamics and kinetics of the homogeneous redox reactions occurring either in the electrolyte solution or on the electrode surface, by means of voltammetric methods. For this reason voltammetry is becoming a widely applied and powerful method for studying the redox cycles occurring in living organisms [1–10]. Second, in

* Corresponding author. Tel.: +389 2 3117 055; fax: +389 2 3226 865.
E-mail address: valentin@iunona.pmf.ukim.edu.mk (V. Mirčeski).

0022-0728/$ - see front matter © 2005 Elsevier B.V. All rights reserved.
doi:10.1016/j.jelechem.2004.12.017

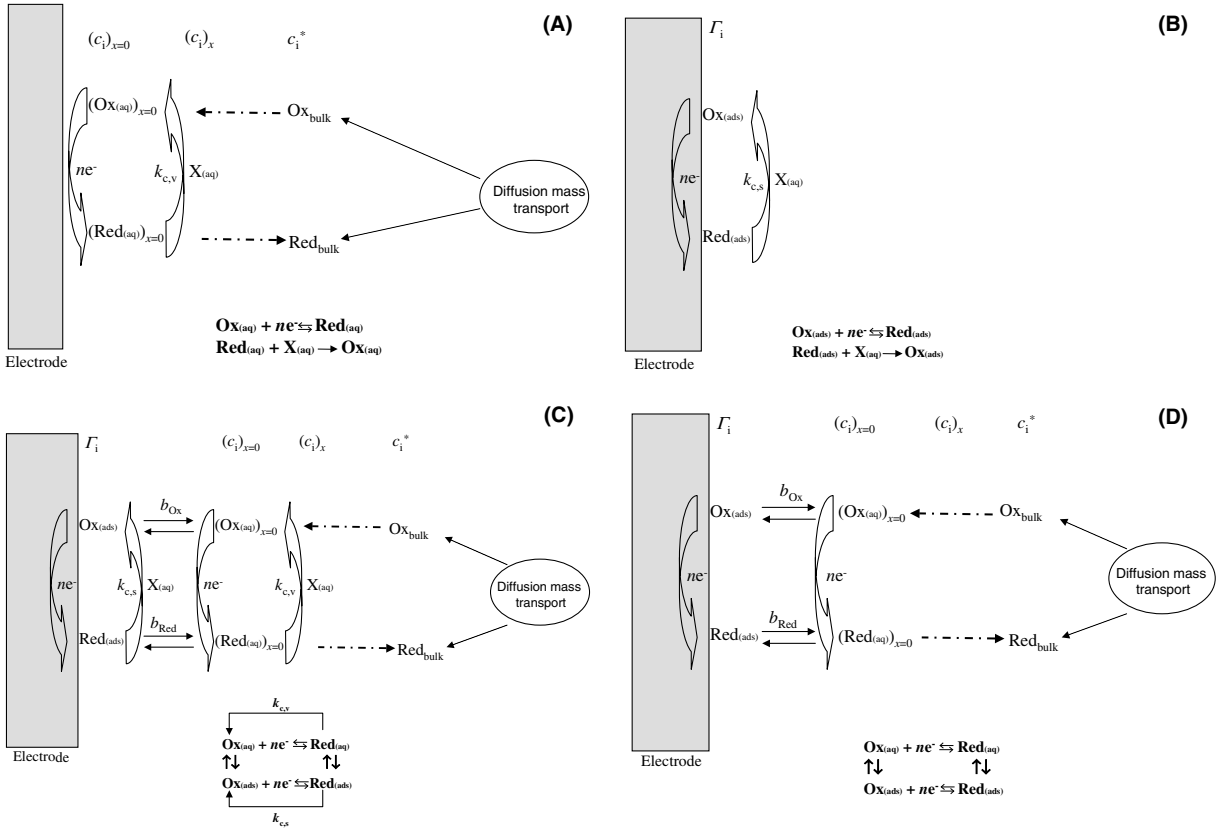

Scheme 1. (A) Reaction scheme for a simple catalytic electrode mechanism of a dissolved redox couple. (B) Reaction scheme for a surface catalytic electrode mechanism of an adsorbed redox couple. (C) Reaction scheme for a catalytic electrode mechanism of a partly adsorbed redox couple. (D) Reaction scheme for an electrode mechanism of a partly adsorbed redox couple.

the catalytic electrode mechanism the electrons are shuttled from the electrode to the species in the electrolyte solution that otherwise are electrochemically inactive or undergo direct electron exchange with the electrode at higher overpotentials. In this sense, the term "catalytic" is appropriate since the product of the heterogeneous electrode reaction acts as a catalyst for the redox transformation of certain species present in the electrolyte solution by lowering their energy of redox transformation. Third, catalytic electrode mechanisms are of particular importance for electroanalytical methods since they increase the ratio of the faradaic and capacitive current I_f/I_c, by increasing the faradaic component, and hence enhance the sensitivity of a particular method [11–16]. The catalytic electrode mechanism is becoming a particularly powerful analytical tool in combination with pulse voltammetric techniques and adsorptive accumulation of the electroactive species [11,17–28]. For these reasons, understanding the role of adsorption in the case of the catalytic mechanism is of crucial importance for optimization of an analytical procedure that utilizes both the catalytic reaction and adsorptive accumulation for amplifying the sensitivity of the method. Besides the analytical utility, the role of adsorption is also important in cases when the catalytic mechanism is applied for studying biologically, macromolecules that adsorb frequently on the electrode surface.

In the theory of voltammetric methods there is a lack of systematic studies considering the role of adsorption in the electrode reactions coupled with homogeneous chemical reactions. The remarkable theoretical work of Laviron et al. [29–34] provided a theoretical basis for understanding surface electrode reactions coupled with chemical reactions mainly under conditions of linear sweep voltammetry. The surface electrode mechanism is the case of very strong irreversible adsorption, when all species are firmly bounded to the electrode surface, excluding the adsorption equilibria and the mass transport of the electroactive species in the course of the voltammetric experiment (see Scheme 1(B)) [35,36]. Nevertheless, the role of adsorption equilibria of the redox couple on the voltammetric properties of the catalytic electrode mechanism is still uncertain. For these reasons, the objective of the current study is to examine theoretically the complex catalytic electrode mechanism coupled by adsorption equilibria of both species of the redox couple (see Scheme 1(C)). In such an electrode mechanism, two electrode reactions have to be considered, i.e., the surface electrode reaction occurring between the adsorbed forms of the redox couple and the

volume electrode reaction occurring between the dissolved forms of the redox couple at the electrode surface. Accordingly, in a general theoretical model concerned with the catalytic mechanism, besides the mass transfer and the adsorption equilibria, two different catalytic reactions have to be considered, i.e., the surface and volume homogeneous redox chemical reactions, characterized with the surface $k_{c,s}$ and volume $k_{c,v}$ rate constants, respectively (see Scheme 1(C)). The results in this study will demonstrate how critical is the type of the catalytic reaction. Both catalytic mechanisms of a dissolved redox couple (Scheme 1(A)) and the surface catalytic mechanism (Scheme 1(B)) are only limiting cases of the general electrode mechanism coupled by adsorption equilibria (Scheme 1(C)).

The electrode mechanism (Scheme 1(C)) is studied by means of square-wave voltammetry (SWV) due to the well-known suitability of this technique for studying adsorption coupled electrode mechanisms [37]. In recent studies we have shown how critical is the role of adsorption in the behaviour of the electrode mechanism followed by homogeneous chemical reactions under conditions of SWV [38,39]. The aim of the present study is to reveal the role of adsorption in the voltammetric behaviour of the catalytic mechanism and its implication towards the sensitivity of the analytical method based on such an electrode mechanism. Second, an attempt is made to establish simple diagnostic criteria for recognition of the nature of the homogeneous redox reaction. Characterization of the inherent nature of the homogeneous redox reaction is of crucial importance for correct estimation of the kinetics of the reaction by means of voltammetric methods.

The theoretical results presented in this paper are verified by the experiments performed with the well-known redox couple azobenzene/hydrazobenzene [35–37,40,41], in the presence of chlorate and bromate ions, as catalytic reagents.

2. Mathematical model

Assuming semi-infinite diffusion at a planar electrode, the electrode mechanism presented in Scheme 1(C) is described by the following set of differential equations:

$$\frac{\partial c_{Ox}}{\partial t} = D\frac{\partial^2 c_{Ox}}{\partial x^2} + k_{c,v}c_{Red}, \tag{1}$$

$$\frac{\partial c_{Red}}{\partial t} = D\frac{\partial^2 c_{Red}}{\partial x^2} - k_{c,v}c_{Red}. \tag{2}$$

Here $k_{c,v}$ (s^{-1}) is the rate constant of the volume catalytic reaction. Most frequently, $k_{c,v}$ is a pseudo first-order chemical rate constant defined as $k_{c,v} = k^*_{c,v}c^*_X$, where $k^*_{c,v}$ is the real second-order rate constant in units of $mol^{-1}\,cm^3\,s^{-1}$ and c^*_X is the concentration of a certain reactant X, i.e., the oxidant in mechanism (Scheme 1(C)), present in an excess, whose concentration is virtually constant in the course of the voltammetric experiment. For the meaning of all other symbols and abbreviations see Table 1. The above equations should be solved under the following initial and boundary conditions:

$$t = 0,\ x \geqslant 0: \quad c_{Ox} = c^*_{Ox},\ c_{Red} = 0,\ \Gamma_{Ox} = \Gamma_{Red} = 0, \tag{a}$$

$$t > 0,\ x \to \infty: \quad c_{Ox} \to c^*_{Ox},\ c_{Red} \to 0, \tag{b}$$

$$x = 0: \quad D\left(\frac{\partial c_{Ox}}{\partial x}\right)_{x=0} = \frac{I}{nFS} + \frac{d\Gamma_{Ox}}{dt} + k_{c,s}\Gamma_{Red}, \tag{c}$$

Table 1
List of symbols and abbreviations

a	auxiliary adsorption parameter
b	common adsorption constant
β	dimensionless adsorption parameter
c^*_{Ox}	bulk concentration of the oxidized form
c^*_X	bulk concentration of the reactant X
$(c_{Ox})_{x=0}$	concentration of the oxidized form at the electrode surface
$(c_{Red})_{x=0}$	concentration of the reduced form at the electrode surface
D	common diffusion coefficient
dE	potential step
E	potential of the working electrode
$E_{acc.}$	accumulation potential
E_{SW}	pulse height
$E^{\emptyset}_{Ox/Red}$	standard redox potential
F	Faraday constant
f	frequency
Φ	auxiliary function
I	current
ΔI_p	real net peak current
$k_{c,s}$	first-order rate constant of the surface catalytic reaction
$k^*_{c,s}$	second-order rate constant of the surface catalytic reaction
$k_{c,v}$	first-order rate constant of the volume catalytic reaction
$k^*_{c,v}$	second-order rate constant of the volume catalytic reaction
n	number of electrons
R	gas constant
S	electrode surface area
T	temperature
t	time
$t_{acc.}$	accumulation time
Γ_{Ox}	surface concentration of the oxidized form
Γ_{Red}	surface concentration of the reduced form
$\kappa_{c,s}$	dimensionless surface catalytic rate parameter
$\kappa_{c,v}$	dimensionless volume catalytic rate parameter
x	distance from the electrode surface
Ψ	dimensionless current
$\Delta\Psi_p$	dimensionless net peak current

$$D\left(\frac{\partial c_{\mathrm{Red}}}{\partial x}\right)_{x=0} = -\frac{I}{nFS} + \frac{\mathrm{d}\Gamma_{\mathrm{Red}}}{\mathrm{d}t} - k_{\mathrm{c,s}}\Gamma_{\mathrm{Red}}, \quad \text{(d)}$$

$$b(c_{\mathrm{Ox}})_{x=0} = \Gamma_{\mathrm{Ox}}, \quad \text{(e)}$$

$$b(c_{\mathrm{Red}})_{x=0} = \Gamma_{\mathrm{Red}}. \quad \text{(f)}$$

Here $k_{\mathrm{c,s}}$ (s^{-1}) is the rate constant of the surface catalytic first-order chemical reaction. By analogy with the volume chemical reaction, one can assume that the surface reaction proceeds also as a pseudo first-order process according to the following scheme: $\mathrm{Red}_{(\mathrm{ads})} + \mathrm{X}_{(\mathrm{aq})} \rightarrow \mathrm{Ox}_{(\mathrm{ads})}$. The latter reaction is of a heterogeneous nature and hence its rate is expressed in units of mol cm^{-2} s^{-1} and it is characterized by a rate constant $k^*_{\mathrm{c,s}}$ in units of mol^{-1} cm^3 s^{-1}. Accordingly, the surface catalytic rate constant $k_{\mathrm{c,s}}$ is assumed to be of pseudo-first order defined as $k_{\mathrm{c,s}} = k^*_{\mathrm{c,s}}c^*_{\mathrm{X}}$, where c^*_{X} is the constant concentration of the reactant X present in an excess. Of course, one could presume that the surface chemical reaction could proceed as a homogeneous process in which both reactants Red and X are adsorbed at the electrode surface. Such a case will increase the complexity of the system at a level beyond the capability of the present model. Under such conditions, the surface chemical reaction has to be treated as a second-order reaction, making impossible, modelling with the aid of Laplace transformations. Therefore, the following derivation is not valid for such a case.

For further simplification, the diffusion coefficients of both Ox and Red species are supposed to be equal. The electrode is under conditions of a low surface coverage, and there are no significant interactions between the adsorbed species. Thus, the adsorption equilibria of both Ox and Red forms can be described with a linear adsorption isotherm law. For most experimental systems these requirements can be easily fulfilled by adjusting the volume concentration of the electroactive reactant, accumulation time, and composition of the supporting electrolyte solution. It is also important to note that a common adsorption constant of both Ox and Red species is assumed. In other words, both Ox and Red forms of the redox couple are adsorbed equally on the electrode surface. Assuming different adsorption constants will make the model mathematically intractable.

To solve Eq. (1) the following substitution is introduced:

$$\Phi = c_{\mathrm{Ox}} + c_{\mathrm{Red}}. \quad (3)$$

Derivatization of the latter equation with respect to the variable t, and considering Eqs. (1) and (2), leads to

$$\frac{\partial \Phi}{\partial t} = D\frac{\partial^2 \Phi}{\partial x^2}. \quad (4)$$

The Eq. (4) is to be solved for the following initial and boundary conditions:

$$t = 0,\ x \geqslant 0: \quad \Phi = c^*_{\mathrm{Ox}},\ \Gamma_\Phi = 0, \quad \text{(g)}$$

$$t > 0,\ x \rightarrow \infty: \quad \Phi \rightarrow c^*_{\mathrm{Ox}}, \quad \text{(h)}$$

$$x = 0: \quad D\left(\frac{\partial \Phi}{\partial x}\right)_{x=0} = \frac{\mathrm{d}\Gamma_\Phi}{\mathrm{d}t}, \quad \text{(i)}$$

$$b\Phi_{x=0} = \Gamma_\Phi, \quad \text{(j)}$$

where $\Gamma_\Phi = \Gamma_{\mathrm{Ox}} + \Gamma_{\mathrm{Red}}$.

Applying the Laplace transform to Eq. (3) and the boundary conditions (g–j), one obtains the following solution:

$$\Phi_{x=0} = c^*_{\mathrm{Ox}}\left\lfloor 1 - \exp\left(a^2 t\right)\mathrm{erfc}\left(a\sqrt{t}\right)\right\rfloor, \quad (5)$$

where $a = \sqrt{D}/b$. The procedure for deriving Eq. (5) is similar to that used in the modeling of a simple electrode reaction coupled by the adsorption of the reactant only [42]. A combination of Eqs. (3) and (5) yields

$$(c_{\mathrm{Ox}})_{x=0} = c^*_{\mathrm{Ox}}\left\lfloor 1 - \exp\left(a^2 t\right)\mathrm{erfc}\left(a\sqrt{t}\right)\right\rfloor - (c_{\mathrm{Red}})_{x=0}. \quad (6)$$

Thus, to obtain the final solution for the concentration of the Ox form at the electrode surface, one requires the solution for the Red form, which can be obtained independently by solving Eq. (2). The boundary value problem for Eq. (2) is equivalent as in the case of an adsorption coupled EC mechanism involving two different follow-up chemical reactions. The solution was recently derived in detail [39]. The solution reads

$$\begin{aligned}(c_{\mathrm{Red}})_{x=0} = {} & \frac{a}{p-q} \\ & \times \int_0^t \frac{I(\tau)}{nFS\sqrt{D}}\left[p\exp\left(p(t-\tau)\right) - q\exp\left(q(t-\tau)\right)\right]\mathrm{d}\tau \\ & - \frac{ak_{\mathrm{c,s}}}{p-q}\int_0^t \frac{I(\tau)}{nFS\sqrt{D}}\left[\exp\left(p(t-\tau)\right)\right. \\ & \left. + \exp\left(q(t-\tau)\right)\right]\mathrm{d}\tau - \frac{a^2}{p-q}\int_0^t \frac{I(\tau)}{nFS\sqrt{D}} \\ & \times \left[\sqrt{k_{\mathrm{c,v}}+p}\ \mathrm{erf}\left(\sqrt{(k_{\mathrm{c,v}}+p)(t-\tau)}\right)\right]\mathrm{d}\tau \\ & + \frac{a^2}{p-q}\int_0^t \frac{I(\tau)}{nFS\sqrt{D}}\left[\sqrt{k_{\mathrm{c,v}}+q}\right. \\ & \left. \times \mathrm{erf}\left(\sqrt{(k_{\mathrm{c,v}}+q)(t-\tau)}\right)\right]\mathrm{d}\tau, \end{aligned} \quad (7)$$

where $p = (B - \sqrt{B^2 - 4C})/2$ and $q = (B + \sqrt{B^2 - 4C})/2$. Here $B = 2k_{\mathrm{c,s}} + a^2$ and $C = k^2_{\mathrm{c,s}} - a^2 k_{\mathrm{c,v}}$.

Finally, we assume that the overall electrode mechanism appears reversible and the Nernst equation holds

$$(c_{\mathrm{Ox}})_{x=0} = (c_{\mathrm{Red}})_{x=0}\exp(\varphi), \quad (8)$$

where $\varphi = nF(E - E^{\emptyset}_{\mathrm{Ox/Red}})/RT$ is the dimensionless potential. Substituting Eqs. (6) and (7) into (8), one easily obtains the solution for a reversible electrode reaction in the form of an integral equation. The solution in the form of an integral equation relates the current with time at a certain potential. Thus, it is a general solution valid for any voltammetric technique. The final numeri-

cal solution of the integral equation depends on the particular voltammetric technique.

In this study, the numerical solution is adopted for SWV. It is obtained according to the standard procedure of the Nicholson and Olmstead method [43]. For numerical integration, a time increment $d = 1/(50f)$ was used, where f is the frequency of the potential modulation. This means that each SW half-period was divided into 25 time increments. An Osteryoung-type of square-wave potential modulation was used, which is a train of negative and positive pulses superimposed to a staircase potential ramp [37]. The signal is characterized with amplitude E_{sw}, which is a half of the peak to peak height, frequency of the pulses f, and potential step of the staircase ramp dE. The theoretical results are expressed in the form of dimensionless current defined as $\psi = I/nFSc^*_{Ox}\sqrt{Df}$.

3. Experimental

All chemicals used were of analytical reagent grade (''Merck'' products). All solutions were prepared with MilliQ water. 0.5 mol/L acetate buffer solution at pH 4.7 was used as a supporting electrolyte. Solutions of $KClO_3$ and $KBrO_3$ were used as oxidants. The stock solution of azobenzene was prepared by dissolving it in glacial acetic acid. Extra pure nitrogen was used for purging the electrolyte solutions for 10 min prior to each measurement. A nitrogen blanket, over the electrolyte solution, was maintained thereafter.

All voltammetric measurements were performed with an Autolab PGSTAT12/GPES (General Purpose Electrochemical System-Version 4.8, Eco Chemie) computer controlled electrochemical system. A hanging mercury drop electrode (HMDE) Metrohm model 663 VA with a mercury drop size of 0.52 mm^2 was used. All potentials are referred to a Ag|AgCl|3 mol/L KCl, reference electrode. The counter electrode was a platinum wire. The quartz voltammetric cell was thermostated at 25 ± 0.1 °C during the experiments in order to maintain reproducible conditions.

4. Results and discussion

4.1. Theoretical results

The electrode mechanism under study consists of two separate electrode reactions, i.e., the surface electrode reaction occurring between the adsorbed species and the volume electrode reaction occurring between the dissolved species at the electrode surface. The two electrode reactions are interconnected with the adsorption equilibria and they both contribute to the overall voltammetric response. Since the adsorption constant is the same for both Ox and Red forms, both electrode reactions are characterized with the same formal potential, thus occurring simultaneously at the same electrode potential. The overall electrode mechanism is predominantly controlled by the strength of the adsorption of the redox couple that is represented by the adsorption constant b, and the rates of the two catalytic reactions, reflected through the rate constants $k_{c,v}$ and $k_{c,s}$. However, the voltammetric response depends on the more complex dimensionless adsorption parameter $\beta = \sqrt{D}/b\sqrt{f}$ and the dimensionless kinetic parameters $\kappa_{c,v} = k_{c,v}/f$ and $\kappa_{c,s} = k_{c,s}/f$. The overall adsorption effect on the voltammetric response is controlled by the position of the adsorption equilibrium, the mass transfer of the electroactive species, and the time window of the voltammetric experiment, whereas, the effect of the catalytic reactions depends on the ratio between the rate constants and the time window of the voltammetric experiment represented by the frequency of the potential modulation.

Fig. 1 shows the effect of the volume catalytic reaction on the dimensionless net SW peak currents for different adsorption strengths of the redox couple, keeping the effect of the surface catalytic reaction negligible. Contrary to the expected behaviour of the catalytic mechanism, the net peak currents are constant over the wide range of values for the volume catalytic rate constant and decrease for the fast volume catalytic reaction. Only for very low values of the adsorption equilibrium constant, when the adsorption of the redox couple can be neglected, can the increase of the current be observed (see curve 5 in Fig. 1). However, under such conditions, the electrode mechanism is equivalent to the simple catalytic mechanism of the dissolved redox couple (see Scheme 1(A)). Fig. 1 shows that, in the presence of different adsorption strengths of the redox couple, the volume catalytic reaction causes a decrease of the net peak current. It can be also noted that as the adsorption becomes stronger, the system is less sensitive to the volume catalytic reaction. At the same time, the peak potential and the half-peak width do not change significantly. Before providing any explanation for such unusual behaviour of the system, it is interesting to examine the effect of the surface catalytic reaction.

Fig. 2 shows the effect of the surface catalytic reaction on the dimensionless net SW peak currents. Obviously, the effect of the surface reaction is completely different in comparison with the volume catalytic reaction. When the surface catalytic reaction commences affecting the SW response, the net peak current increases dramatically, reaching a maximum value at a certain critical rate of the surface reaction. Above this critical surface reaction rate, the net peak current diminishes steeply. Thus, a sharp maximum is observed in the dependence of the net peak current versus the logarithm of the surface reaction rate constant. The position of this maximum is dependent on the adsorption strength. As the

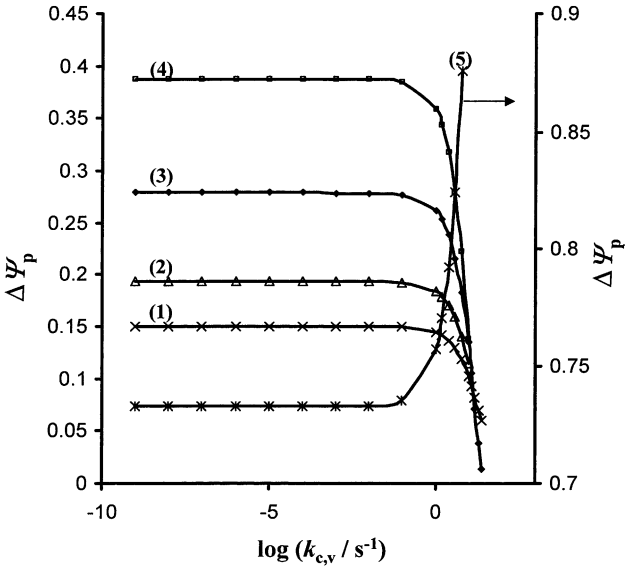

Fig. 1. The dependence of the net peak current on the logarithm of the volume catalytic rate constant for different adsorption strengths of the redox couple. The adsorption constant was: $b = 0.033$ (1); 0.02 (2); 0.01 (3) and 0.005 cm (4). Curve 5 (right ordinate) refers to the catalytic mechanism in the absence of adsorption (Scheme 1(A)). The other simulation conditions were: $nE_{sw} = 50$ mV, $dE = 5$ mV, $t_{acc.} = 0$ s, $E_{acc.} = 0.15$ V versus $E^{\emptyset}_{Ox/Red}$, log ($k_{c,s}$/$s^{-}1$) = −8, and $f = 10$ Hz.

adsorption decreases, the maximum shifts towards higher surface reaction rate constants. The position of each maximum is associated with a certain critical value of the surface rate constant $(k_{c,s})_{max}$. Interestingly, there is an exact linear dependence of the logarithms of the adsorption constant and $(k_{c,s})_{max}$. The inset of Fig. 2 shows this dependence, which is described by the following linear regression line: $\log[(k_{c,s})_{max}/s^{-1}] = -2.1101 \log(b/cm) - 5.4062$. The importance of this equation follows from the fact that it enables determination of the surface catalytic rate constant if the adsorption equilibrium constant of the redox couple is known. The latter relationship stems from the fact that the overall rate of the surface catalytic reaction depends on both the rate constant and the surface concentration of the $Red_{(ads)}$ form that is controlled by the adsorption equilibrium. For weaker adsorption, thus a higher rate constant is required to reach the same maximum as for stronger adsorption.

In order to reveal some of the reasons causing such a remarkable effect of the surface catalytic reaction, it is advisable to inspect the shape of all components of the SW voltammetric response. Fig. 3 shows SW voltammograms simulated for a single adsorption constant of $b = 0.033$ cm and different rates of the surface reaction. The voltammograms correspond to the curve 1 in Fig. 2. The voltammogram in Fig. 3(a) refers to the slow surface reaction when its effect is insignificant to the overall catalytic electrode mechanism. The shape of the voltammetric curves is typical for an adsorption coupled electrode reaction [44]. The voltammograms in Fig. 3(b) correspond to the conditions close to the maximum effect of the surface catalytic reaction. It is important to emphasize that the shape of the forward and backward components is not sigmoidal, as expected for a catalytic reaction. Both components are intensive bell-shaped curves characteristic for a surface electrode reaction. Obviously, under such conditions, the overall voltammetric response of the complex catalytic mechanism originates mainly from the surface electrode reaction. For higher rates of the surface reaction (see Fig. 3(c)) the bell-shaped curves are transformed into sigmoidal curves, as expected for a catalytic reaction. However, in spite of the fast catalytic reaction, the overall current values are strongly diminished in comparison to the voltammograms in Fig. 3(b).

The foregoing remarkable behaviour of the system is a consequence of the simultaneous influence of several factors such as: (i) the specific chronoamperometric properties of the adsorption coupled electrode mechanism (ii) the specific potential modulation used in SWV and the current sampling procedure, (iii) the presence of chemical reactions that regenerate the electroactive material during the voltammetric experiment, and (iv) the rate of the mass transport process. To understand the complex behaviour of the system under study, we must recall the electrode mechanism coupled by adsorption of the redox couple only (see Scheme 1(D)).

From the chronoamperometry of an adsorbed redox couple, it is known that the current diminishes with time more severely than for a dissolved redox couple. It is also known that in SWV, the current is sampled at the end of each potential pulse. For an adsorbed redox couple, a low current portion remains to be measured at the end of the potential pulse due to a fast establishment of the redox equilibrium between the adsorbed species. For these reasons, for an electrode mechanism coupled by adsorption only (see Scheme 1(D)), the net SW current decreases as the adsorption of the redox couple increases. The occurrence of both the volume and surface catalytic reactions has two important consequences: first, both reactions re-supply the electrode surface with the electroactive material, and second, probably more important, affect all the equilibria of the electrode mechanism, thus causing changes in the chronoamperometric properties of the system. For instance, the action of the surface catalytic reaction prevents rapid establishment of the redox equilibrium between the $Ox_{(ads)}/Red_{(ads)}$ couple during a single potential pulse and hence causes an increase of the net peak current. However, the decrease of the surface concentration of the $Red_{(ads)}$ form affects the adsorption equilibrium $Red_{(aq)} \leftrightarrow Red_{(ads)}$ shifting it towards the right hand side. Actually, though the $Red_{(ads)}$ form is permanently transformed into $Ox_{(ads)}$, for sufficiently strong adsorption (approximately $\log(b) > -1.8$) the diminishing of its surface con-

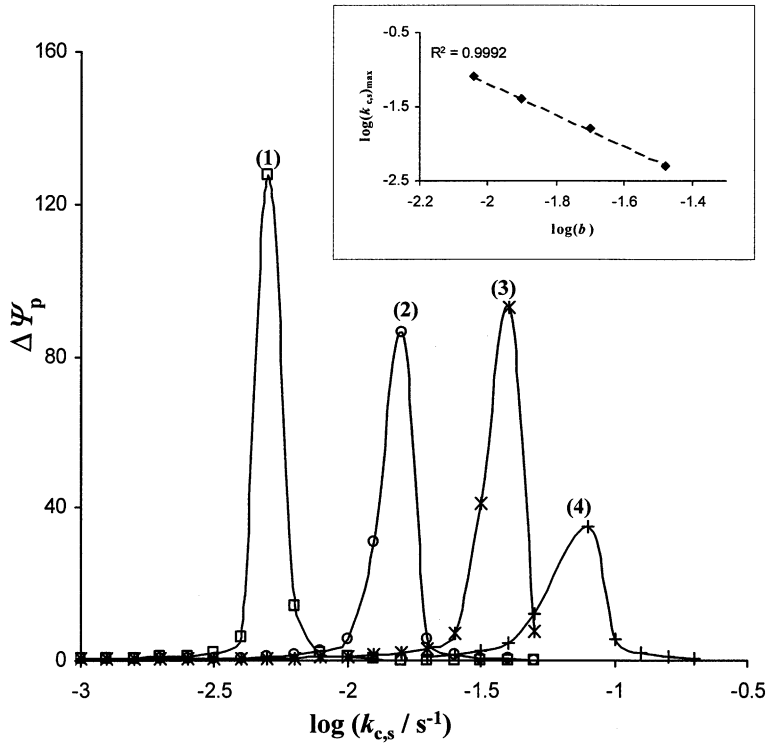

Fig. 2. The dependence of the net peak current on the logarithm of the surface catalytic rate constant for different adsorption strengths of the redox couple. The adsorption constant was: $b = 0.033$ (1); 0.02 (2); 0.0125 (3) and 0.009 cm (4). The other simulation conditions were: $nE_{sw} = 50$ mV, $dE = 10$ mV, $t_{acc.} = 10$ s, $E_{acc.} = 0.15$ V versus $E^{\emptyset}_{Ox/Red}$, log ($k_{c,v}$/s^{-1}) = −8, and $f = 10$ Hz. The inset shows the dependence of the critical values of the surface catalytic rate constant on the adsorption constant.

centration is prevented by the latter equilibrium, which in turn amplifies the effect of the surface catalytic reaction. It appears that under certain conditions, the surface catalytic reaction regenerates the adsorbed reactant without losing the $Red_{(ads)}$ form. For these reasons, the surface catalytic reaction enhances both the forward and backward components of the SW response simultaneously (see the voltammograms in Fig. 3(b)).

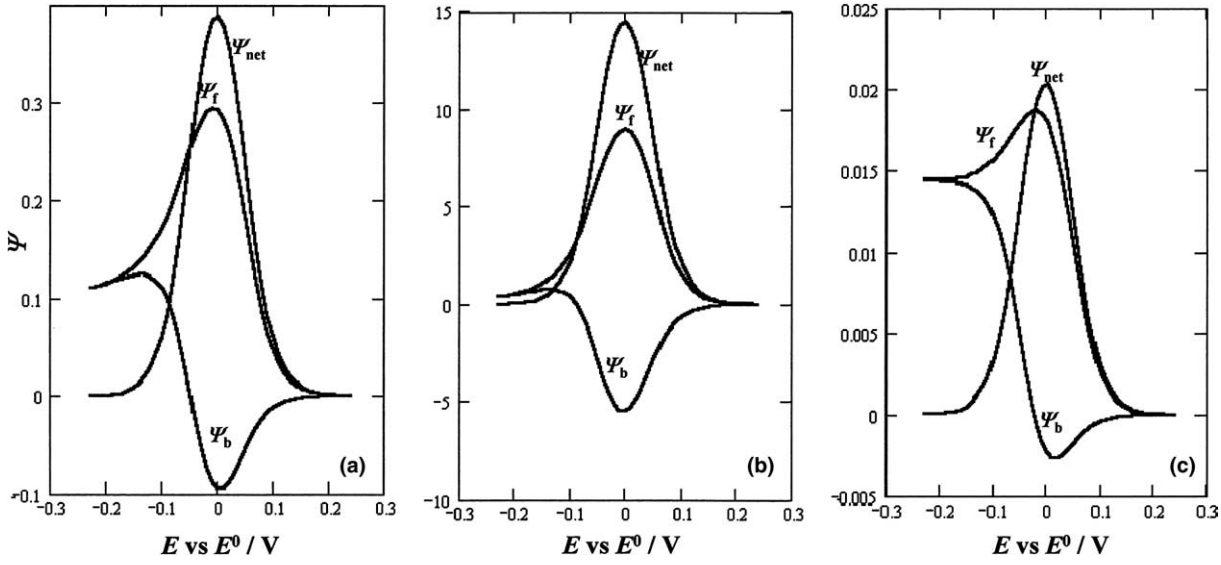

Fig. 3. The effect of the surface catalytic rate constant on all components of the SW voltammetric response. The surface catalytic rate constant was: log ($k_{c,s}$/s^{-1}) = −3 (a); −2.2 (b) and −1 (c). The other conditions of the simulations were: $b = 0.033$ cm, $nE_{sw} = 50$ mV, $dE = 10$ mV, $t_{acc.} = 10$ s, $E_{acc.} = 0.15$ V versus $E^{\emptyset}_{Ox/Red}$, log ($k_{c,v}$/s^{-1}) = −8, and $f = 10$ Hz. The subscripts: net, f, and b, correspond to the net, forward and backward components of the SW response, respectively.

Further on, the right-hand shift of the $Red_{(aq)} \leftrightarrow Red_{(ads)}$ prevents the establishment of the redox equilibrium between the dissolved redox couple $Ox_{(aq)}/Red_{(aq)}$ that also contributes to the increase of the overall current. Therefore, when the rate of the surface catalytic reaction is synchronized with the adsorption equilibria, the duration of the SW potential pulses, and the rate of the mass transfer of the dissolved electroactive species, an exhaustive reuse of the electroactive material occurs on the electrode surface causing a dramatic increase of the current.

When the surface catalytic reaction is very fast, the $Red_{(aq)} \leftrightarrow Red_{(ads)}$ cannot succeed re-supplying the electrode surface with the $Red_{(ads)}$ form and the forward and backward components gain a sigmoidal shape, as expected for a catalytic reaction (see Fig. 3(c)). However, the current values are strongly diminished and the system behaves similarly to a fast chemically irreversible electrode process of an immobilized reactant.

A repetitive reuse of the electroactive material cannot be achieved due to the volume catalytic reaction. Although the volume chemical reaction regenerates the $Ox_{(aq)}$ form, it affects the adsorption equilibria in a manner that produces a decrease of the current. The decrease of the $Red_{(aq)}$ form due to the volume catalytic reaction affects $Red_{(aq)} \leftrightarrow Red_{(ads)}$ causing a complete exhaustion of the $Red_{(ads)}$ form, as its absolute amount on the electrode surface is very low. As a consequence, the backward components of both the volume and surface electrode reactions do not develop and consequently they do not contribute to the overall net response. On the other hand, although the $Ox_{(aq)}$ form is regenerated, a significant portion of it is lost through the adsorption equilibrium $Ox_{(aq)} \leftrightarrow Ox_{(ads)}$. It follows that the effect of the volume catalytic reaction is equivalent to that of a very fast surface reaction. Again the system behaves similarly to the fast and chemically irreversible electrode reaction of a strongly adsorbed reactant, which produces a low current.

The foregoing results clearly demonstrate the difference in the influence of the surface and volume catalytic reaction. In the real experiment, the inspection of the net peak current versus the concentration of the catalytic agent, together with the analysis of the shape of the complete voltammetric response, can reveal which type of catalytic reaction predominates. Furthermore, it is shown that partial adsorption of the redox couple plays a critical role in the behaviour of the catalytic electrode mechanism. The consequences of such an electrode mechanism towards the sensitivity of an analytical method under conditions of SWV are straightforward. In this context, Fig. 4 shows the variation of the net peak current with the adsorption constant for different rate constants of the surface catalytic reaction. Obviously, moderate adsorption is favourable for reaching the maximal sensitivity of the method. Both pure surface and volume catalytic mechanisms (see Schemes 1(A) and (B)) are inferior in comparison with the adsorption coupled catalytic mechanism from an analytical point of

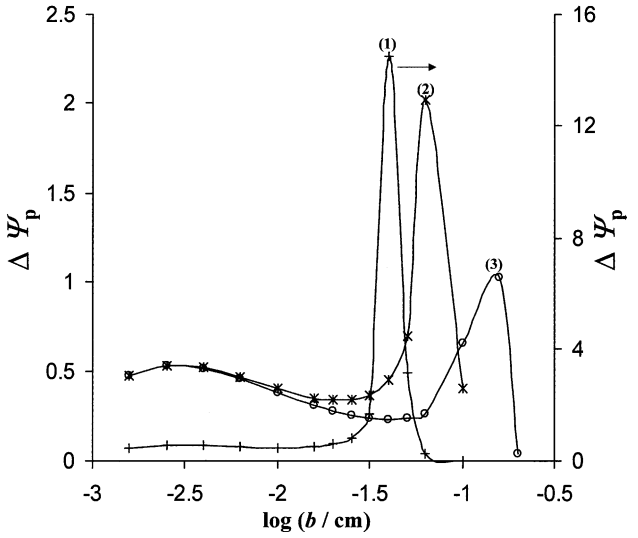

Fig. 4. The dependence of the net peak current on the logarithm of the adsorption constant for different rates of the surface catalytic reaction. The rate constant of the surface catalytic reaction was: $\log (k_{c,s}/s^{-1}) = -2$ (1); -3 (2) and -3.5 (3). The other simulation conditions were the same as in Fig. 2. The curve 1 refers to the right ordinate.

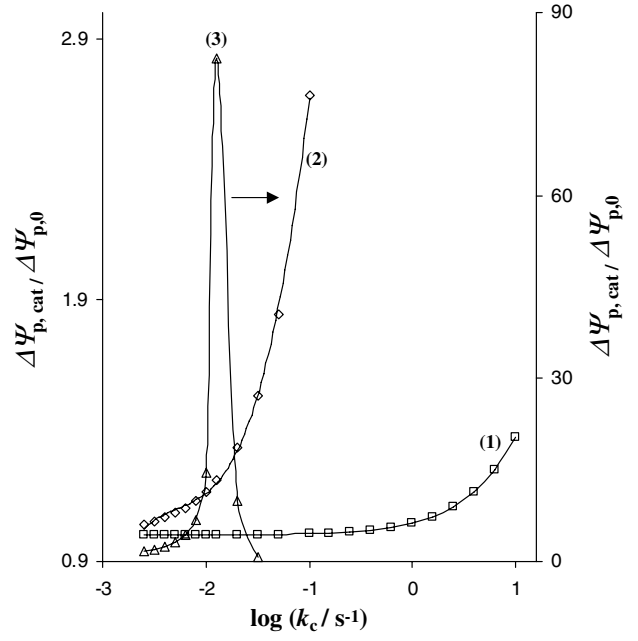

Fig. 5. A comparison of the effect of the catalytic reaction on the net peak current of a catalytic mechanism of a dissolved redox couple (curve 1, Scheme 1(A)), surface catalytic mechanism (curve 2, Scheme 1(B)), and an adsorption coupled catalytic reaction (curve 3, Scheme 1(C)). The simulation conditions were: $nE_{sw} = 10$ mV and $dE = 10$ mV. In the case of the adsorption coupled catalytic mechanism (curve 3), the adsorption constant was $b = 0.02$ cm and the volume catalytic rate constant was $\log (k_{c,v}/s^{-1}) = -8$. Curve 3 refers to the right ordinate.

view. Fig. 5 compares the relative increases of the peak currents with the rates of the catalytic reaction for all three mechanisms. For consistent comparison, the ordinate displays the ratio $\Delta\Psi_{p,cat}/\Delta\Psi_{p,0}$, where $\Delta\Psi_{p,cat}$ and $\Delta\Psi_{p,0}$ are the peak currents of the catalytic mechanism and the corresponding mechanism in the absence of the catalytic reaction, respectively. The analytical utility of the adsorption coupled catalytic electrode mechanism is obvious.

4.2. Experimental results

The theoretically predicted phenomena are illustrated experimentally by the voltammetric properties of the electrode reaction of azobenzene at the hanging mercury drop electrode. The electrode reaction of azobenzene has been studied extensively and used for illustration of a different adsorption coupled electrode mechanisms [35–37,40–42]. It undergoes a chemically reversible two-electron and two-proton reduction to hydrazobenzene. In an aqueous medium, both azobenzene and hydrazobenzene are strongly adsorbed on the mercury electrode surface and the electrode mechanism exhibits the properties of a surface process. In the presence of an organic solvent such as acetonitrile (ACN), the electrode reaction can be transposed into the mechanism of a partly adsorbed redox couple. In the presence of an oxidant, such as chlorate or bromate, the electrode reaction is transposed into a catalytic electrode mechanism in which the hydrazobenzene is reoxidized back to azobenzene by means of a homogeneous redox reaction. The rate of the catalytic reaction is controlled by the concentration of the oxidant in the electrolyte solution, whereas the strength of adsorption is inversely proportional to the content of ACN in the electrolyte.

Fig. 6 depicts the influence of the chlorate ions on the net SW peak current of azobenzene for a series of measurements performed in an acetate buffer containing different amounts of ACN. In a pure aqueous medium, when the azobenzene/hydrazobenzene redox couple is strongly adsorbed on the electrode surface, the increasing chlorate concentration caused only a slight decrease of the current (see curve 1 in Fig. 6). Interestingly, in a medium where the adsorption is weaker, increasing the concentration of chlorate caused an increase of the net peak current. In media containing 25%, 40% and 50% (v/v) ACN, parabola-shape dependences were found (see curves 3–5 in Fig. 6) supporting the theoretical predictions. The positions of these experimental maxima are dependent on the ACN content. The maximum is shifted

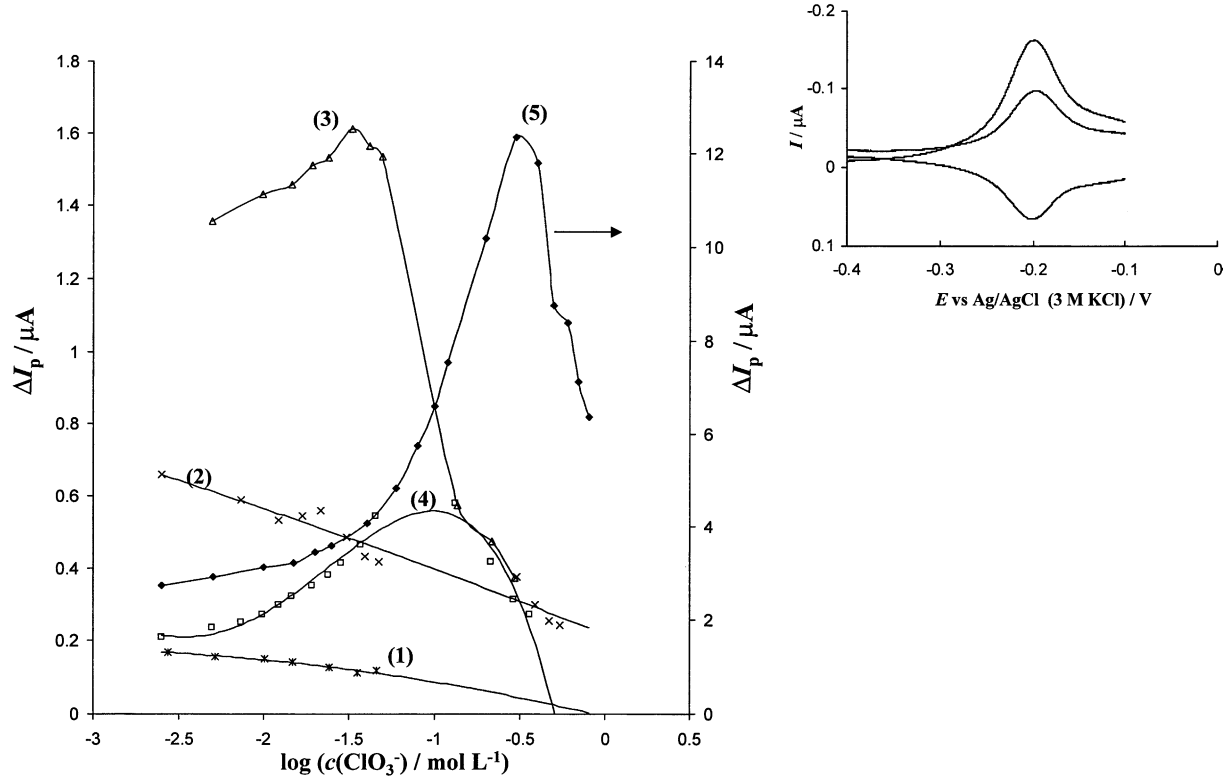

Fig. 6. The effect of chlorate ions on the net peak current of azobenzene recorded in acetate buffer at pH 4.75 containing different amount of acetonitrile (ACN). The content of ACN expressed in volumic parts was: 0% (1); 11% (2); 25% (3); 40% (4) and 50% (5). The other experimental conditions were: azobenzene concentration 1×10^{-6} mol/L, $t_{acc.} = 15$ s, $E_{acc.} = -0.100$ V, $E_{SW} = 20$ mV, $dE = 0.1$ mV, and $f = 60$ Hz. The accumulation was performed with stirring for curves 2–4. The inset shows the SW voltammograms of azobenzene corresponding to the maximum of the curve 5.

towards higher chlorate concentrations by increasing the ACN content. Keeping in mind that the adsorption strength decreases with increasing ACN content, these experimental findings are in agreement with the predicted effect of the adsorption on the position of the maxima due to the occurrence of the surface catalytic reaction (see Fig. 2). It must be emphasized that the experimental situation is much more complex than that considered theoretically. Besides affecting the adsorption strength, ACN could also affect the activity of chlorate, thus additionally changing the rate of the catalytic reaction for a particular chlorate concentration.

The inset of Fig. 6 depicts complete SW voltammograms of azobenzene corresponding to the maximum of the curve 5. Obviously, the maximal current is not a consequence of the sigmoidal forward and backward SW components. Both components are bell-shaped symmetrical peaks with almost identical peak heights and potentials. The shapes of these experimental voltammograms of azobenzene resemble the theoretical voltammograms in Fig. 3(b). Therefore, all these results indicate that the catalytic reaction of azobenzene in the presence of ACN and chlorate is of a surface nature.

Similar results have been found using bromate ions as an oxidant (see Fig. 7). The maximum was observed in a medium containing 10% ACN. In a medium containing 50% ACN the current increases rapidly with the bro-

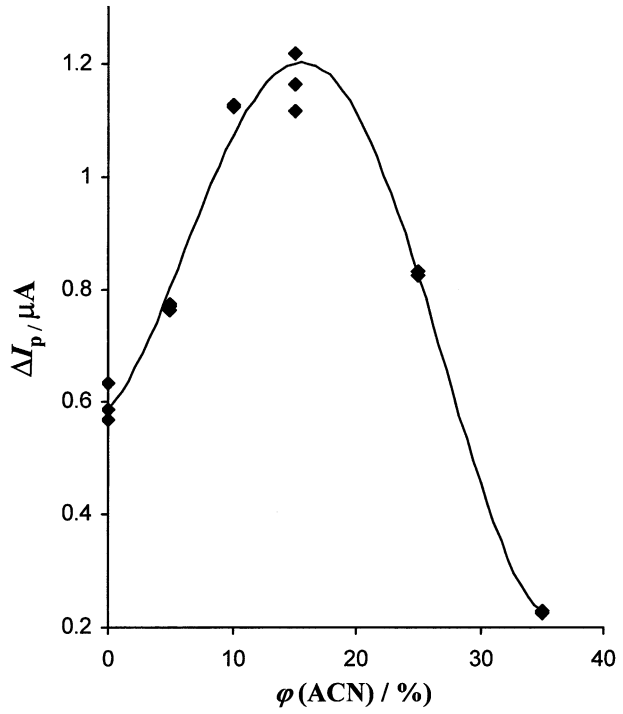

Fig. 8. The effect of the acetonitrile content on the net peak current of azobenzene recorded in the presence of 2.38×10^{-3} mol/L chlorate ions in the supporting electrolyte. The other conditions were the same as in Fig. 6. The accumulation was performed by stirring of the solutions.

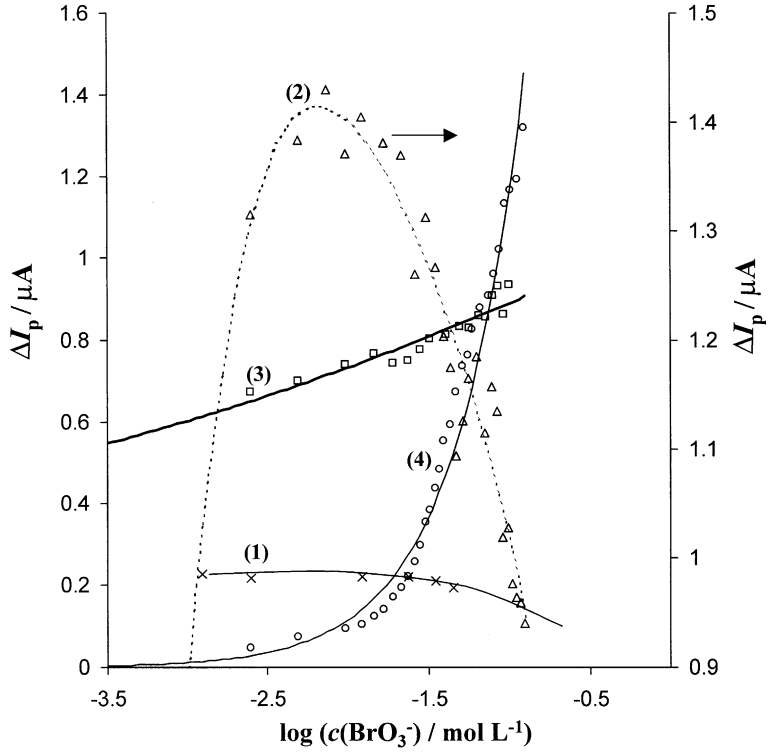

Fig. 7. The effect of bromate ions on the net peak current of azobenzene recorded in acetate buffer at pH 4.75 containing different amounts of acetonitrile. The content of ACN expressed in volumic parts was: 0% (1); 10% (2); 25% (3) and 50% (4). The other experimental conditions were the same as in Fig. 6. The accumulation was performed by stirring of the solutions.

mate concentration, although the adsorption in such medium is the weakest. The experiment is limited with the maximal solubility of bromate ions, which is not sufficient to reach the maximum of the current.

To illustrate the theoretical results presented in Fig. 4, showing the effect of adsorption in the presence of surface catalytic reaction, series of measurements have been carried out by changing the content of acetonitrile and keeping the concentration of the oxidant at a constant level. Fig. 8 shows that the net peak current of azobenzene depends parabolically on the amount of ACN, reaching the maximum at 15% of ACN for 2.38×10^{-3} mol/L concentration of chlorate ions. These experiments confirm that at particular rate of the surface catalytic reaction the moderate adsorption will provides the highest sensitivity of the method, in agreement with the prediction of the theoretical results in Fig. 4.

5. Conclusion

To the best of our knowledge this is the first theoretical study revealing the role of adsorption in the catalytic electrode mechanism based on a rigorous mathematical modelling. The complex electrode mechanism considered involves two types of catalytic reactions, i.e., surface and volume catalytic reactions. It is demonstrated that square-wave voltammetry is a powerful technique, able to distinguish between these two catalytic reactions. Under particular conditions, when the rate of the surface catalytic reaction is synchronized with the adsorption equilibria and mass transport rate, a repetitive reuse of the electroactive material at the electrode surface occurs, causing a dramatic increase of the SW voltammetric response. Based on this property, the catalytic electrode mechanism of moderate adsorption of the redox couple would provide the highest analytical sensitivity in comparison to catalytic mechanisms of a dissolved redox couple or pure surface mechanism.

Acknowledgements

V.M. gratefully acknowledges the financial support of both A. v. Humboldt-Stiftung and Université de Bretagne Occidentale.

References

[1] C. Leger, S.J. Elliot, K.R. Hoke, L.J.C. Jeunken, A.K. Jones, F.A. Armstrong, Biochemistry 42 (2003) 8653.
[2] J. Di, S. Bi, M. Zhang, Biosensors Bioelectron. 19 (2004) 1479.
[3] L. Dennany, R.J. Forster, J.F. Rusling, J. Am. Chem. Soc. 125 (2003) 5213.
[4] P. Tomcik, E.C. Banks, J.T. Davies, R.G. Compton, Anal. Chem. 76 (2004) 161.
[5] L. Zhou, J.F. Rusling, Anal. Chem. 73 (2001) 4780.
[6] A. Mugweru, J.F. Rusling, Anal. Chem. 74 (2002) 4044.
[7] L. Trnkova, R. Kizek, J. Vacek, Bioelectrochemistry 56 (2002) 57.
[8] H. Huang, N. Hu, Y. Zeng, G. Zhou, Anal. Biochem. 308 (2002) 141.
[9] E. Lojou, P. Bianco, Electrochim. Acta 47 (2002) 4069.
[10] H. Liu, N. Hu, Anal. Chim. Acta. 481 (2003) 91.
[11] A. Bobrowski, J. Zarebski, Electroanalysis 12 (2000) 1177.
[12] H. He, K. Siow, H. Chi, Z. Gao, A. Hsieh, Anal. Chim. Acta 309 (1995) 73.
[13] R. Inam, G. Somer, Talanta 50 (1999) 609.
[14] J. Wang, B. Serra, S.Y. Ly, J. Lu, J.M. Pingarron, Talanta 54 (2001) 147.
[15] C. Sun, Q. Gao, J. Xi, H. Xu, Anal. Chim. Acta 309 (1995) 89.
[16] Z. Jiang, L. Liao, M. Liu, Anal. Chim. Acta 300 (1995) 107.
[17] B. Magyar, H.R. Elsener, S. Wunderli, Microchim. Acta III (1990) 179.
[18] A. Harbin, C.M.G. van den Berg, Anal. Chem. 65 (1993) 3411.
[19] M. Vega, C.M.G. van den Berg, Anal. Chem. 69 (1997) 874.
[20] Z. Gao, K.S. Siow, Electroanalysis 8 (1996) 602.
[21] A. Bobrowski, A.M. Bond, Electroanalysis 4 (1992) 975.
[22] M. Gawrys, J. Golimowski, Anal. Chim. Acta 427 (2001) 55.
[23] A. Safavi, E. Shams, Talanta 51 (2000) 1117.
[24] Z. Gao, K.S. Siow, Talanta 43 (1996) 255.
[25] H. Obata, C.M.G. van den Berg, Anal. Chem. 73 (2001) 2522.
[26] K. Yokoi, C.M.G. van den Berg, Anal. Chim. Acta 245 (1991) 167.
[27] J. Wang, J. Lu, Z. Taha, Analyst 117 (1992) 35.
[28] P.A.M. Farias, A.K. Ohara, A.W. Nobrega, J.S. Gold, Electroanalysis 6 (1994) 333.
[29] E. Laviron, J. Electroanal. Chem. 35 (1972) 333.
[30] E. Laviron, J. Electroanal. Chem. 42 (1973) 415.
[31] E. Laviron, J. Electroanal. Chem. 391 (1995) 187.
[32] E. Laviron, R. Meunier-Prest, R. Lacasse, J. Electroanal. Chem. 375 (1994) 263.
[33] R. Meunier-Prest, E. Laviron, J. Electroanal. Chem. 437 (1997) 61.
[34] E. Laviron, L. Roullier, Electrochim. Acta 18 (1973) 237.
[35] V. Mirčeski, R. Gulaboski, J. Solid State Electrochem. 7 (2003) 157.
[36] V. Mirčeski, R. Gulaboski, Electroanalysis 13 (2001) 1326.
[37] M. Lovrić, in: F. Scholz (Ed.), Electroanalytical Methods, Guide to Experiments and Applications, Springer-Verlag, Berlin, Heidelberg, 2002, pp. 111–133.
[38] V. Mirčeski, J. Electroanal. Chem. 508 (2001) 138.
[39] V. Mirčeski, M. Lovrić, J. Electroanal. Chem. 565 (2004) 191.
[40] R.H. Wopschall, I. Shain, Anal. Chem. 39 (1967) 1535.
[41] R.P. Van Duyne, T.H. Ridgway, C.N. Reilley, J. Electroanal. Chem. 34 (1972) 283.
[42] M. Lovrić, M. Branica, J. Electroanal. Chem. 226 (1987) 239.
[43] R.S. Nicholson, M.L. Olmstead, in: J.S. Mattson, H.B. Mark, H.C. Macdonald (Eds.), Electrochemistry: Calculations, Simulation and Instrumentation, vol. 2, Marcel-Dekker, New York, 1972, pp. 120–137.
[44] M. Lovrić, Š. Komorsky-Lovrić, J. Electroanal. Chem. 248 (1988) 239.